

Effects of individual heterogeneity on social contagions

Fu-Zhong Nian(年福忠) and Yu Yang(杨宇)

Citation: Chin. Phys. B, 2024, 33 (**5**): 058705. DOI: 10.1088/1674-1056/ad225e

What follows is a list of articles you may be interested in

Studying the co-evolution of information diffusion, vaccination behavior and disease transmission in multilayer networks with local and global effects

Liang'an Huo(霍良安) and Bingjie Wu(武兵杰)

Chin. Phys. B, 2024, 33 (**3**): 038702. DOI: 10.1088/1674-1056/ad0114

Impact of individual behavior adoption heterogeneity on epidemic transmission in multiplex networks

Liang'an Huo(霍良安) and Yue Yu(于跃)

Chin. Phys. B, 2023, 32 (**10**): 108703. DOI: 10.1088/1674-1056/acea65

Drop impact on substrates with heterogeneous stiffness

Yang Cheng(成阳), Jian-Gen Zheng(郑建艮), Chen Yang(杨晨), Song-Lei Yuan(袁松雷), Guo Chen(陈果), and Li-Yu Liu(刘雳宇)

Chin. Phys. B, 2022, 31 (**8**): 084702. DOI: 10.1088/1674-1056/ac5c33

The most common friend first immunization

Fu-Zhong Nian(年福忠), Cha-Sheng Hu(胡茶升)

Chin. Phys. B, 2016, 25 (**12**): 128702. DOI: 10.1088/1674-1056/25/12/128702

Detecting overlapping communities in networks via dominant label propagation

Sun He-Li (孙鹤立), Huang Jian-Bin (黄健斌), Tian Yong-Qiang (田勇强), Song Qin-Bao (宋擒豹), Liu Huai-Liang (刘怀亮)

Chin. Phys. B, 2015, 24 (**1**): 018703. DOI: 10.1088/1674-1056/24/1/018703

Effects of individual heterogeneity on social contagions

Fu-Zhong Nian(年福忠)[†] and Yu Yang(杨宇)

School of Computer and Communication, Lanzhou University of Technology, Lanzhou 730000, *China*

(Received 18 November 2023; revised manuscript received 22 January 2024; accepted manuscript online 25 January 2024)

Despite having significant effects on social contagions, individual heterogeneity has frequently been overlooked in earlier studies. To better understand the complexity of social contagions, a non-Markovian model incorporating heterogeneous social influence and adoption thresholds is introduced. For theoretical analysis, a generalized edge-based compartmental theory which considers the heterogeneities of social influence and adoption thresholds is developed. Focusing on the final adoption size, the critical propagation probability, and the phase transition type, social contagions for adoption thresholds that follow normal distributions with various standard deviations, follow various distributions, and correlate with degrees are investigated. When thresholds follow normal distributions, a larger standard deviation results in a larger final adoption size when the information propagation probability is relatively low. However, when the information propagation probability is relatively high, a larger standard deviation results in a smaller final adoption size. When thresholds follow various distributions, crossover phenomena in phase transition are observed when investigating the relationship of the final adoption size versus the average adoption threshold for some threshold distributions. When thresholds are correlated with degrees, similar crossover phenomena occur when investigating the relationship of the final adoption size versus the degree correlation index. Additionally, we find that increasing the heterogeneity of social influence suppresses the effects of adoption threshold heterogeneity on social contagions in three cases. Our theory predictions agree well with the simulation results.

Keywords: complex networks, social contagions, heterogeneity, phase transition.

PACS: 87.23.Ge, 87.23.Kg, 05.90.+m, 89.75.−k **DOI:** 10.1088/1674-1056/ad225e

1. Introduction

Spreading is one of the most significant dynamical processes in complex networks, involving epidemic spreading, information diffusion, behavior propagation, innovation dissemination, and more. Scholars have broadly classified spreading dynamics as either biological contagions or social contagions. Epidemic spreading is a fundamental type of biological contagion referred to as a simple contagion, in which a virus is transmitted by each contact with the same probability, and the effects of each contact are independent of each other. Information diffusion and behavior propagation belong to social contagions, also known as complex contagions.[1–3] There are extensive social reinforcement effects in social contagions,[4–6] where the effects of multiple contacts work cumulatively, making social contagions fundamentally different from biological contagions.

Threshold models are widely used for studying social contagions. Granovetter[7] proposed a threshold model, in which an individual adopts a new opinion once the proportion of his closest neighbors who adopt the opinion is larger than an assigned threshold. Complex non-linear collective behavior phenomena emerge in this model. Watts[8] proposed a threshold model that makes decisions based on the total number of neighbors who adopt the behavior. The effects of one randomly selected initiator on the final cascade size are investigated in this paper. Moreover, many scholars proposed corresponding threshold models for specific social contagions and numerous phase transition phenomena are observed.[9–12] However, these earlier studies tend to assume that all individuals have the same social influence and an identical adoption threshold, neglecting the effects of individual heterogeneity.

Recently, scholars have focused on the effects of heterogeneity on the spreading dynamics. For epidemic spreading, heterogeneous infectivity and susceptibility will change the outbreak threshold.[13,14] In information diffusion, the heterogeneous waiting time and response time can speed up or slow down the velocity of information spreading.[15,16] Zhu has shown that degree heterogeneity can not only alter the nature of contagions' transition from discontinuous to continuous but also can increase or decrease the final adoption size.[17] Wang proposed a threshold model based on heterogeneous credibility and found that the final adoption size versus the heterogeneity parameter exhibits a discontinuous pattern.[18] Wang also proposed a threshold model that considers the heterogeneity of adoption thresholds, categorizing individuals as either activists with lower thresholds or bigots with higher thresholds, and discovered crossover phenomena in phase transition by varying the threshold and the proportion of the activists.[19] Karampourniotis also introduced a model which considers the heterogeneity of adoption thresholds and studied the effects of the initiator set size on the final adoption size.[20]

This paper investigates the effects of individual heterogeneity on social contagions, and two types of individual heterogeneity are considered: One is the heterogeneity of adop-

[†]Corresponding author. E-mail: gdnfz@lut.edu.cn

© 2024 Chinese Physical Society and IOP Publishing Ltd

tion thresholds. Individuals' attitudes towards the same information vary due to their interests, educational backgrounds, and other social factors, resulting in heterogeneous adoption thresholds.[21,22] Another is the heterogeneity of social influence. For instance, celebrities have greater social influence while the social influence of ordinary people is comparatively much weaker.[23] Referring to Ref. [24], a generalized non-Markovian model for social contagions is proposed, which considers both heterogeneous social influence and heterogeneous adoption thresholds. Inspired by the edge-based compartmental theory[18,25] and the heterogeneous mean-field theory,[26,27] a generalized edge-based compartmental theory considering the heterogeneity of social influence and adoption thresholds is developed for theoretical analysis. Then, a series of simulations are conducted to investigate the effects of heterogeneous social influence and heterogeneous adoption thresholds on social contagions. For heterogeneous social influence, it is assumed to be positively correlated with degrees from a macroscopic perspective. For heterogeneous adoption thresholds, three scenarios are considered. In the first scenario (Subsection 4.1), heterogeneous adoption thresholds are drawn from a truncated normal distribution, and the effects of mean and standard deviation of adoption thresholds on social contagions are investigated. In the second scenario (Subsection 4.2), the effects of seven different types of threshold distributions on social contagions are investigated. The adoption thresholds are uncorrelated with degrees in the above two scenarios. In the last scenario (Subsection 4.3), we investigate the social contagions when adoption thresholds are positively or negatively correlated with degrees. All the three scenarios focus on the final adoption size, the critical information propagation probability for outbreaks, and their dependence on the dynamical parameters. Besides, the phase transition type and crossover phenomena are investigated.

2. Model descriptions

This paper hypothesizes that social influence is positively correlated with degrees from a macroscopic perspective. To simplify the study, the social influence of individual i with degree k is defined as follows:

$$E_k = k^{\alpha}, \tag{1}$$

where α denotes the heterogeneity parameter of social influence. $\alpha > 0$ so that high-degree individuals have high social influence; the larger its value, the stronger the social influence of individuals with a specific degree.

A generalized susceptible–adopted–recovered (SAR) model is developed to describe the dynamics of social contagions.[28] The states of individuals are classified as susceptible (S), adopted (A), and recovered (R). Individuals in the susceptible state have not adopted the behavior. Those in the adopted state have adopted the behavior and will try to propagate the behavior information to their neighbors. Meanwhile, individuals in the recovered state have lost interest in the behavior, and they will no longer propagate the behavior information.

Initially, a small proportion ρ_0 of individuals are randomly selected as seed adopters, and the remaining individuals are set in the susceptible state. Adoption thresholds can be categorized into two cases. In one case, adoption thresholds are assumed to be uncorrelated with degrees, and the adoption thresholds are set according to a given distribution. The adoption threshold for individual j is denoted by T_j, and the proportion of individuals with an adoption threshold of T is denoted by $F(T)$. In another case, the adoption threshold of an individual is assumed to be correlated with his degree. The adoption thresholds are determined by a given function $f(k)$. The adoption threshold for individual j satisfies $T_j = f(k_j)$, where k_j denotes the degree of individual j. In this paper, $f(k)$ is defined as follows:

$$f(k) = \frac{NT_0 k^{\beta}}{\sum_j {k_j}^{\beta}}, \tag{2}$$

where N denotes the number of all individuals, T_0 denotes the expected average adoption threshold, and β denotes the degree correlation index. When $\beta > 0$, high-degree individuals have a high adoption threshold. The opposite is the case when $\beta < 0$. All individuals have an identical adoption threshold of T_0 when $\beta = 0$.

At each time step, individuals in the adopted state will propagate the behavior information to their susceptible neighbors with probability λ. Once the information has been successfully propagated via an edge, the edge will never propagate the information again, causing only non-redundant information propagation to be allowed. We denote the cumulative influence on a susceptible individual j at time step t as $C_j(t)$, which represents the sum of the social influence on individual j up to time step t. When an individual j newly receives the behavior information from an adopted neighbor i at time step t, the cumulative influence on him will increase E_{k_i}. Individual j will become adopted as soon as $C_j(t) \geq T_j$. In addition, individuals will lose interest and shift to the recovered state with probability γ at each time step. The spreading dynamics terminate when there are no adopted individuals in the system. Since whether an individual adopts the behavior is determined by the cumulative influence that he has ever received, the proposed model is a non-Markovian model.

3. Theoretical approach

Inspired by the edge-based compartmental theory[18,25] and the heterogeneous mean-field theory,[26,27] a general-

ized edge-based compartmental theory which considers both heterogeneous social influence and heterogeneous adoption thresholds is developed for theoretical analysis. In the theory framework, we define $\theta_{k'}(t)$ to denote the probability that individual i with degree k' has not propagated the information via a randomly selected edge to neighbor j up to time t. Besides, we assume that individual j is in a cavity state, meaning that he cannot propagate information to his neighbors, but can receive information from them.

The probability that an individual with degree k has not received the information from a randomly selected neighbor by time t can be calculated by

$$\eta_k(t) = \sum_{k'} P_{\mathrm{c}}\left(k'|k\right)\theta_{k'}(t), \tag{3}$$

where the conditional probability $P_{\mathrm{c}}(k'|k)$ denotes the probability that a randomly selected neighbor of an individual with degree k has a degree of k'. Then the probability that an individual with degree k receives m messages by time t can be expressed as

$$\phi(k,m,t) = \binom{k}{m}[\eta_k(t)]^{k-m}[1-\eta_k(t)]^m. \tag{4}$$

Using κ_k to denote the average social influence of the neighbors for individuals of degree k, it is defined as follows:

$$\kappa_k = \sum_{k'} P_{\mathrm{c}}\left(k'|k\right)E_{k'}. \tag{5}$$

For an individual j with degree k and adoption threshold T_j, the probability of remaining susceptible by time t is approximately equal to the probability that the number of messages he has received is less than $\lfloor T_j/\kappa_k \rfloor$. Using $s(k,t)$ to denote the probability that an individual with degree k remains susceptible by time t, when adoption thresholds are uncorrelated with degrees, $s(k,t)$ is equal to

$$s(k,t) = \sum_{T_j} F(T_j) \sum_{m=0}^{\left\lfloor \frac{T_j}{\kappa_k} \right\rfloor} \phi(k,m,t). \tag{6}$$

When adoption thresholds are correlated with degrees, $s(k,t)$ can be calculated by

$$s(k,t) = \sum_{m=0}^{\left\lfloor \frac{f(k)}{\kappa_k} \right\rfloor} \phi(k,m,t). \tag{7}$$

Combined with the degree distribution of the network $P(k)$, we can obtain the probability that a randomly selected individual is in the adopted state at time t as follows:

$$S(t) = (1-\rho_0)\sum_k P(k)\,s(k,t), \tag{8}$$

which also represents the proportion of the adopted individuals at time t. Once the network structure is determined, then the degree distribution $P(k)$ and the conditional probability $P_{\mathrm{c}}(k'|k)$ can be obtained statistically. The distribution of the adoption threshold $F(T)$ or the threshold function $f(k)$ is given. Thus, once $\theta_{k'}(t)$ can be obtained, $S(t)$ can be calculated.

Using $\xi^{\mathrm{S}}_{k'}(t)$ ($\xi^{\mathrm{A}}_{k'}(t)$ or $\xi^{\mathrm{R}}_{k'}(t)$) to denote the probability that a neighbor of i is in the susceptible (adopted or recovered) state and has not propagated the behavior information to individual j up to time t, then $\theta_{k'}(t)$ can be expressed as

$$\theta_{k'}(t) = \xi^{\mathrm{S}}_{k'}(t) + \xi^{\mathrm{A}}_{k'}(t) + \xi^{\mathrm{R}}_{k'}(t). \tag{9}$$

When individual i with degree k' is susceptible initially, he cannot propagate the behavior information to individual j, but can only receive the information from the other $k'-1$ neighbors, since individual j is assumed to be in the cavity state. Thus, in the case that adoption thresholds are uncorrelated with degrees, $\xi^{\mathrm{S}}_{k'}(t)$ can be obtained as follows:

$$\xi^{\mathrm{S}}_{k'}(t) = (1-\rho_0)\sum_{T_i} F(T_i) \sum_{m=0}^{\left\lfloor \frac{T_i}{\kappa_{k'}} \right\rfloor} \phi\left(k'-1,m,t\right). \tag{10}$$

In another case in which adoption thresholds are correlated with degrees, $\xi^{\mathrm{S}}_{k'}(t)$ can be calculated by

$$\xi^{\mathrm{S}}_{k'}(t) = (1-\rho_0) \sum_{m=0}^{\left\lfloor \frac{f(k')}{\kappa_{k'}} \right\rfloor} \phi\left(k'-1,m,t\right). \tag{11}$$

As soon as the behavior information is propagated successfully via an edge with probability λ, this edge will no longer meet the definition of $\theta_{k'}(t)$. So, it can be obtained that

$$\frac{\mathrm{d}\theta_{k'}(t)}{\mathrm{d}t} = -\lambda\xi^{\mathrm{A}}_{k'}(t). \tag{12}$$

For the evolution of $\xi^{\mathrm{R}}_{k'}(t)$, there are two conditions that must be satisfied simultaneously: (i) the adopted individuals have not propagated the information with probability $1-\lambda$ and (ii) the adopted individuals become recovered with probability γ. So, we can obtain

$$\frac{\mathrm{d}\xi^{\mathrm{R}}_{k'}(t)}{\mathrm{d}t} = \gamma\xi^{\mathrm{A}}_{k'}(t)(1-\lambda). \tag{13}$$

Combining the above equations, $\theta_{k'}(t)$ can be obtained, and then we can obtain $S(t)$.

It can be known from the model description in Section 2 that the susceptible individuals will shift to the adopted states after adopting the behavior, while the individuals in the adopted state will lose their interest in the behavior and recover. Thus, the proportion of individuals in the adopted and recovered states at time t can easily be calculated by

$$\frac{\mathrm{d}A(t)}{\mathrm{d}t} = -\frac{\mathrm{d}S(t)}{\mathrm{d}t} - \gamma A(t), \tag{14}$$

$$\frac{\mathrm{d}R(t)}{\mathrm{d}t} = \gamma A(t). \tag{15}$$

Since $S(t)$ has been obtained in the previous paragraphs, we can obtain $A(t)$ and $R(t)$ with Eqs. (14) and (15). The final adoption size $R(\infty)$ can be obtained when $t \to \infty$.

Regarding the critical propagation probability λ_c for outbreaks, here we only analyze its approximation qualitatively. We use the propagation probability that results in the final adoption size satisfying $R(\infty) = 2\rho_0$ as the critical propagation probability. The approximation is very close to the actual value, but slightly larger.

4. Simulation results

All simulations are conducted on BA scale-free networks with network size $N = 10^4$ and average degree $\langle k \rangle = 10$. The proportion of the initial seeds and the recovery probability are set as $\rho_0 = 0.05$ and $\gamma = 1$, respectively. We use 100 fixed networks to conduct the simulations, and 10^3 independent simulations are conducted on each network, then the averages are calculated to be the final simulation results. In this way, we can ensure the reliability of the results and reduce the influence of random factors on the simulations.

4.1. Social contagions with adoption thresholds following normal distributions

In this subsection, both the social influence and the adoption thresholds in the simulations are divided into two cases: heterogeneous and homogeneous. The heterogeneous social influence is calculated by Eq. (1), while the homogeneous social influence is calculated by $E_u = \langle k_u^\alpha \rangle$ to ensure that the average social influence is the same in both homogeneous and heterogeneous cases. For adoption thresholds, in the heterogeneous case, the heterogeneous adoption thresholds are drawn from a truncated normal distribution with mean T_0 and standard deviation σ in interval $[0, 2T_0]$. The left boundary is taken to be 0 to make the adoption threshold greater than or equal to zero, while the right boundary is taken as $2T_0$ so that the average adoption threshold is equal to T_0. We set up four parameter configurations for heterogeneous adoption thresholds: T_0 is fixed at 15, and σ is set at 3, 5, 10, and 50. The smaller σ, the more concentrated the distribution of the adoption thresholds, and when $\sigma = 3$, most adoption thresholds are concentrated around the average. The larger σ is, the more uniformly the adoption thresholds are distributed, and when $\sigma = 50$, the adoption thresholds approximately follow a uniform distribution. The adoption thresholds in the homogeneous case are set by $T_i = T_0$ to ensure that the average adoption thresholds are the same in both homogeneous and heterogeneous cases.

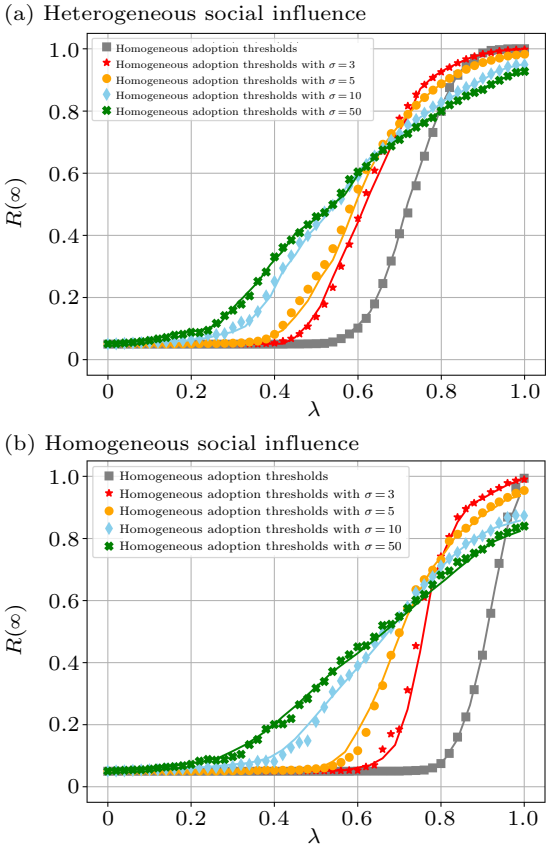


Fig. 1. The final adoption size $R(\infty)$ versus the information propagation probability λ under various conditions. In subgraph (a), the social influence is heterogeneous with $\alpha = 0.25$, while in subgraph (b), the social influence is homogeneous with $\alpha = 0.25$. In both subgraphs, there are five cases representing the homogeneous adoption thresholds and heterogeneous adoption thresholds with $\sigma = 3$, 5, 10, and 50 respectively. T_0 is fixed at 15. The lines are the theoretical predictions, and the dots are the simulation results.

Firstly, we investigate the effects of the information propagation probability λ on the final adoption size $R(\infty)$ under various conditions, and the results are shown in Fig. 1. From Figs. 1(a) and 1(b), we can see that the distribution uniformity of the heterogeneous adoption thresholds has a two-sided effect on social contagions. On the one hand, as σ increases, more uniform adoption thresholds lower the spreading threshold, which shows a promotion effect on social contagions. On the other hand, the larger the σ, the flatter the trend of $R(\infty)$ versus λ becomes, which exhibits an inhibitory effect on social contagions. As a result of the above two-sided effect, the curves with different σ will intersect and a type of crossover phenomenon is observed: To the left of the intersection point, the curve with a larger σ is higher, indicating that when λ is relatively low, the more uniform the adoption thresholds are and the more favorable it is for social contagions. However, to the right of the intersection point the curve with a larger σ is lower, indicating that when λ is relatively high, more uniform adoption thresholds will suppress the social contagions. Comparing Figs. 1(a) and 1(b), for the same adoption threshold distribution, we find that the λ_c in the case of heterogeneous social influence are smaller than those in the case of homoge-

neous social influence, and $R(\infty)$ for the same λ in the case of heterogeneous social influence are larger than those in the case of homogeneous social influence, suggesting that heterogeneous social influence promotes the social contagions.

Next, in the case of heterogeneous social influence, the effects of λ on $R(\infty)$ for different α are investigated, and the results are shown in Fig. 2. As α increases, two phenomena are observed: (i) The curves with different σ are approaching each other, and (ii) the intersection points of these curves are moving to the left. Phenomenon (i) suggests that an increase in α suppresses the effect of σ on social contagions. As shown in Fig. 2(c), when $\alpha = 0.75$, the curves corresponding to the different σ are almost overlapped, indicating that the effect of σ on social contagions becomes insignificant when α is large enough. Phenomenon (ii) will further produce a reversal phenomenon: taking $\lambda = 0.4$ as an example, it can be seen in Fig. 2(a) that a larger σ leads to a larger $R(\infty)$ when $\alpha = 0.25$. However, when $\alpha = 0.5$, Fig. 2(b) shows that a larger σ results in a smaller $R(\infty)$.

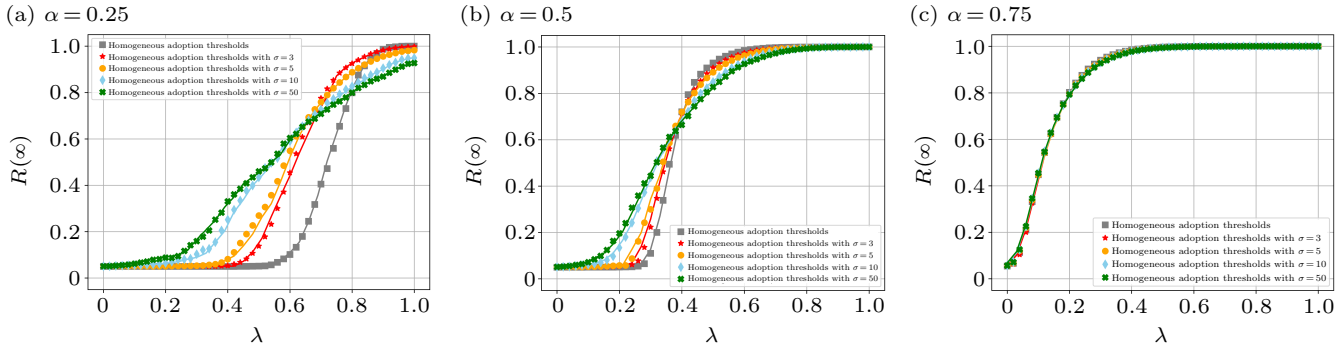


Fig. 2. The final adoption size $R(\infty)$ versus the information propagation probability λ with heterogeneous social influence for different α. The heterogeneity parameters of social influence α in the subgraphs (a), (b), and (c) are 0.25, 0.5, and 0.75, respectively. In each subgraph, there are five cases representing the homogeneous adoption thresholds and heterogeneous adoption thresholds with $\sigma = 3$, 5, 10, and 50. T_0 is fixed at 15. The lines are theoretical predictions, and the dots are simulation results.

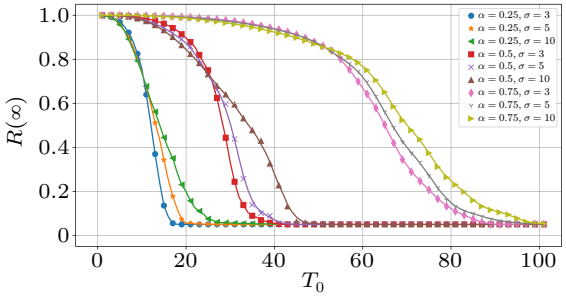


Fig. 3. The final adoption size $R(\infty)$ versus the average adoption threshold T_0 with different α and σ in the case that both social influence and adoption thresholds are heterogeneous while $\lambda = 0.5$. The lines are theoretical predictions, and the dots are simulation results.

Then, we investigate the effects of the average adoption threshold T_0 on the final adoption size $R(\infty)$ when both social influence and adoption thresholds are heterogeneous, and the results are shown in Fig. 3. As can be seen in the figure, the larger the α, the larger the maximum average adoption threshold required for outbreaks, implying that a larger α is more favorable for social contagions. For the cases where α is equal but σ is different, a different type of crossover phenomenon occurs: The curves corresponding to different σ have intersection points. To the left of the intersection point, the curve with a larger σ is lower, indicating that when T_0 is small, a more concentrated threshold distribution is more favorable for social contagions. However, since T_0 is relatively small to the left of the intersection point, the curves with the same α but different σ are close to each other, making the above feature less obvious. To the right of the intersection point, the curve with a larger σ is higher, indicating that when T_0 is large enough, the larger T_0, the more favorable it is for social contagions. When T_0 is larger than the horizontal coordinate of the intersection point, curves with the same α but different σ are further apart, making the above feature more obvious.

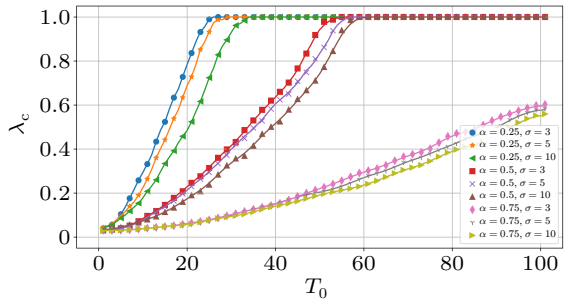


Fig. 4. The critical information propagation probability λ_c versus the mean adoption threshold T_0 with different α and σ in the case that both social influence and adoption thresholds are heterogeneous. The lines are theoretical predictions, and the dots are simulation results.

Lastly, in the case that both social influence and adoption thresholds are heterogeneous, the effects of T_0 on λ_c are investigated, and the results are shown in Fig. 4. The curves with the same α but different σ are closer to each other, while the curves with different α but the same σ are further apart. This indicates that α is the main factor affecting the relationship of λ_c versus T_0, while σ is a secondary factor. Looking at the curves with the same α but different σ, we find that the curve

with a larger σ is lower, which means that the λ_c corresponding to a larger σ is smaller, suggesting that a more uniform threshold distribution is more favorable for social contagions. As α increases, it can be found that curves with the same α but different σ are getting closer, proving that an increase in α suppresses the effect of σ on social contagions once again from another angle.

4.2. The effects of various threshold distributions on social contagions

For the same group of individuals, the threshold distribution may vary with different information. Thus, for some specific information, the threshold distribution is likely to follow other types of distributions other than a normal distribution. With this in mind, we will investigate the effects of various types of threshold distributions on the social contagions. Here, we use seven representative distributions to perform the simulations. Homogeneous thresholds represent the case that all individuals have an identical threshold. The normally distributed thresholds are drawn from a truncated normal distribution in the interval $[0, 2T_0]$ with a mean of 15 and a standard deviation of 5, which is denoted as distribution a for simplicity. There are two cases where adoption thresholds follow truncated power-law distributions with an index of 0.5. In one case, the long tail represents high thresholds, while in the other case, the long tail represents low thresholds. The corresponding adoption thresholds in the above two cases are referred to as distributions b and c for simplicity. The case where adoption thresholds follow uniform distributions in the interval $[0, 2T_0]$ is also considered, and is denoted as distribution d for simplicity. The cases where $F(T)$ decreases or increases linearly as T increases in the interval $[0, 2T_0]$ are denoted as distributions e and f, respectively.

Figure 5 shows the effects of various types of threshold distributions on the relationship of $R(\infty)$ versus λ. When comparing the spreading speeds of the seven types of threshold distributions, we find that the spreading speed corresponding to distribution e is the fastest, while the spreading speed corresponding to distribution c is the slowest. The spreading speed corresponding to the case of homogeneous thresholds is neither the fastest nor the slowest. Besides, we also find that the distribution b is always more favorable for social contagions than the distribution c, and the distribution e is always more favorable for social contagions than the distribution f. The above results imply that a threshold distribution which has more activists with lower thresholds and fewer bigots with higher thresholds is more favorable for social contagions. When α is relatively low, the results corresponding to different threshold distributions show significant differences. However, as α increases, the differences are getting smaller. When $\alpha = 1.25$, the differences almost disappear. Thus, it can be concluded that the increasing of α will suppress the effects of adoption thresholds' heterogeneity on social contagions. This phenomenon can be explained as follows: Use $\langle E_k \rangle$ to denote the average social influence. For individual i with adoption threshold T_i, use $\langle m_i \rangle$ to denote the required average number of messages for him to become adopted, which can be calculated as follows:

$$\langle m_i \rangle = \frac{T_i}{\langle E_k \rangle}. \tag{16}$$

As α increases, social influence will get higher, leading to a higher $\langle E_k \rangle$ and a lower $\langle m_i \rangle$. For individual j with adoption threshold T_j ($T_i > T_j$), the difference between $\langle m_i \rangle$ and $\langle m_j \rangle$ can be calculated as follows:

$$\Delta m_{ij} = \langle m_i \rangle - \langle m_i \rangle = \frac{T_i - T_j}{\langle E_k \rangle}. \tag{17}$$

The Δm_{ij} will decrease with the increasing α. When α is large enough, Δm_{ij} will decrease below 1, causing the effects of adoption threshold heterogeneity to disappear, since the required average numbers of messages for individuals with different adoption thresholds to become adopted are almost identical.

Figure 6 shows the effects of T_0 on $R(\infty)$ for $\alpha = 0.1$, 0.3, and 0.5, while $\lambda = 0.5$. We find that α changes the phase transition type of $R(\infty)$ versus T_0 for some types of threshold distributions. For the cases of homogeneous thresholds,

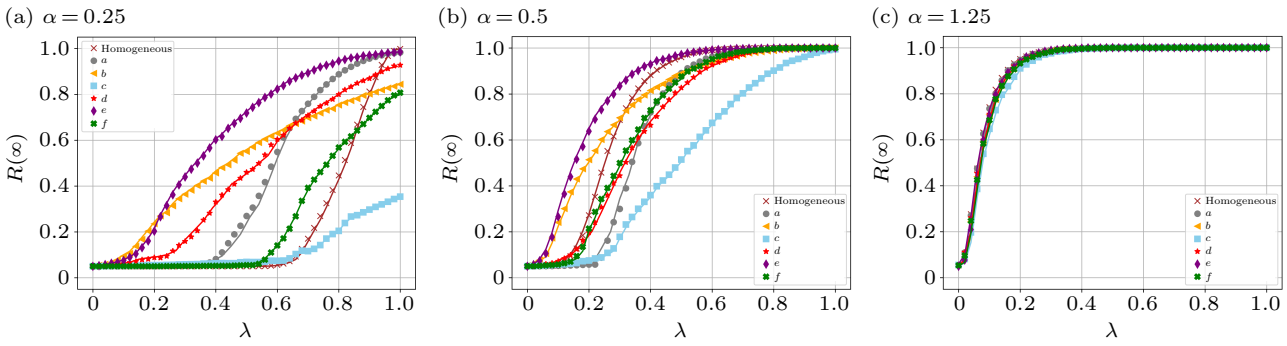


Fig. 5. The final adoption size $R(\infty)$ versus the information propagation probability λ with various types of threshold distributions. The plot of "Homogeneous" represents the result when all adoption thresholds are identical. The plots a–f represent the results corresponding to the threshold distributions a–f, respectively. The lines are theoretical predictions, and the dots are simulation results.

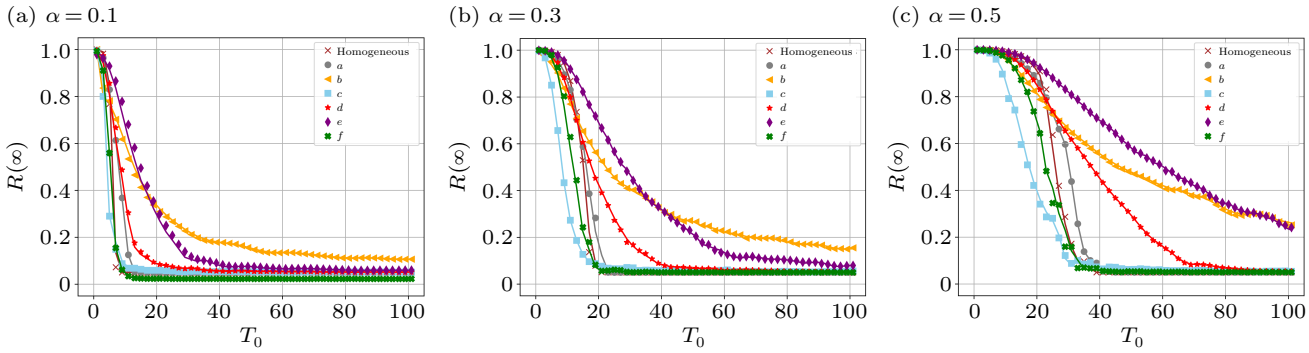


Fig. 6. The final adoption size $R(\infty)$ versus the average adoption threshold T_0 for (a) $\alpha = 0.1$, (b) $\alpha = 0.3$, and (c) $\alpha = 0.5$ while $\lambda = 0.5$. In each subgraph, the plot of "Homogeneous" represents the result when all adoption thresholds are identical, and the plots a–f represent the results corresponding to the threshold distributions a–f, respectively. The lines are theoretical predictions, and the dots are simulation results.

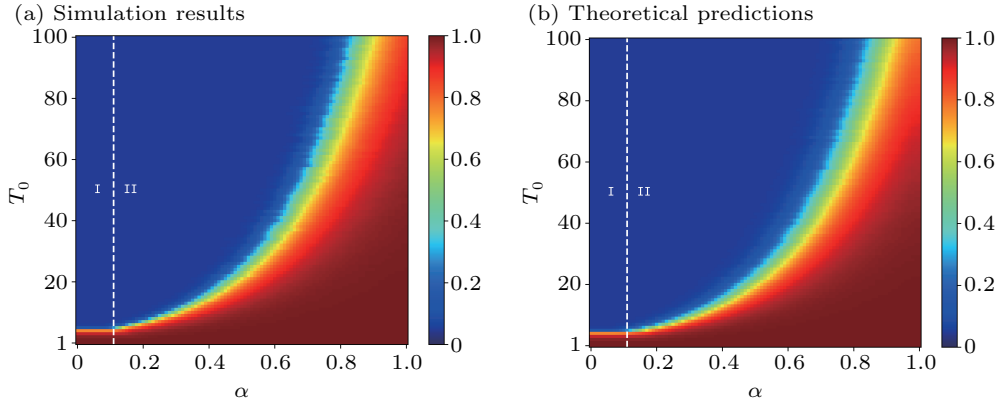


Fig. 7. The dependence of $R(\infty)$ on α and T_0 when the adoption thresholds are homogeneous and $\lambda = 0.5$. Subgraph (a) shows the simulation results, while subgraph (b) shows the theoretical predictions.

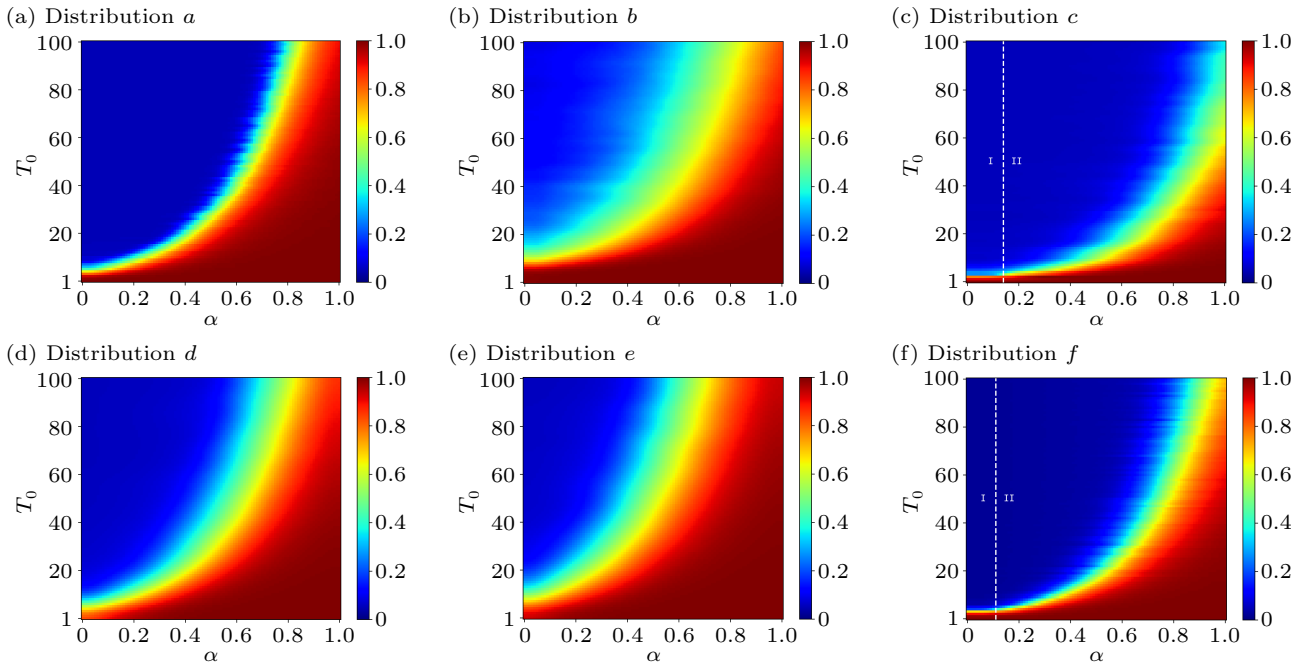


Fig. 8. The dependence of $R(\infty)$ on α and T_0 for distributions a–f while $\lambda = 0.5$.

distribution c, and distribution f, $R(\infty)$ decreases continuously with T_0 for $\alpha = 0.3$ and $\alpha = 0.5$, showing a second-order phase transition. However, when $\alpha = 0.1$, $R(\infty)$ decreases discontinuously with T_0, the phase transition type changes to first-order. To further investigate the above crossover phenomenon in phase transition, we obtain the results of $R(\infty)$ on the α–T_0 plane, which are shown in Figs. 7 and 8. Note that here we only consider the case where $\alpha \in [0,1]$ and $T_0 \in [0,100]$ to simplify the study. Figure 7 shows both the simulation results and the theoretical predictions of $R(\infty)$ on the α–T_0 plane

when the adoption thresholds are homogeneous. The different phase transition regions are separated by the vertical white dashed line. In region I, $R(\infty)$ decreases discontinuously with T_0, showing a first-order phase transition, while in region II, $R(\infty)$ decreases continuously with T_0, showing a second-order phase transition. The theoretical predictions agree well with the simulation results, which demonstrates the validity of our theory. Figure 8 shows the simulation results of $R(\infty)$ on the α–T_0 plane for the other six types of threshold distributions. The same crossover phenomena in phase transition are observed for the cases of distributions c and f. The result implies that social contagions with homogeneous thresholds will exhibit crossover phenomena in phase transition. Moreover, social contagions with numerous bigots who have higher thresholds will also exhibit crossover phenomena in phase transition.

At the end of this subsection, we will investigate the effects of α and T_0 on λ_c, and the results are shown in Figs. 9 and 10. Figure 9 shows the results when the adoption thresholds are homogeneous, and the theoretical predictions agree well with the simulation results again. Figure 10 shows the simulation results of α on the α–T_0 plane for the other six types of threshold distributions. For all the seven types of threshold distributions, there is no sign of crossover phenomena in phase transition. Comparing the effects of the seven types of threshold distributions on λ_c, the distribution b is the most favorable for outbreaks, whatever the value of α and T_0, and the minimum propagation probabilities that outbreaks required are quite small. This is because the distribution b is a power-law distribution with high thresholds representing the long tail. In this case, there are many activists with low thresholds who can easily adopt the behavior. After the activists adopt the behavior, the activists' neighbors are influenced to adopt the behavior, then the social contagion breaks out. The case corresponding to distribution e is similar to the case corresponding to distribution b in that there are also many activists, making it the second most favorable case for outbreaks.

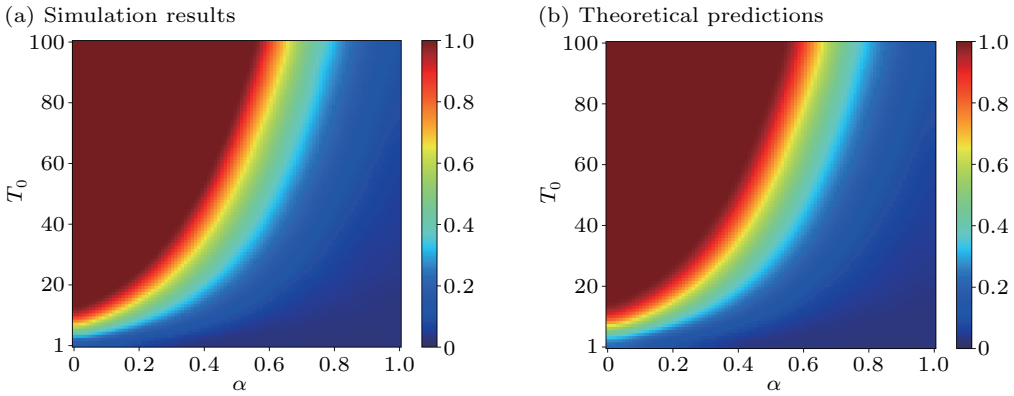


Fig. 9. The dependence of λ_c on α and T_0 when the adoption thresholds are homogeneous. Subgraph (a) shows the simulation results, while subgraph (b) shows the theoretical predictions.

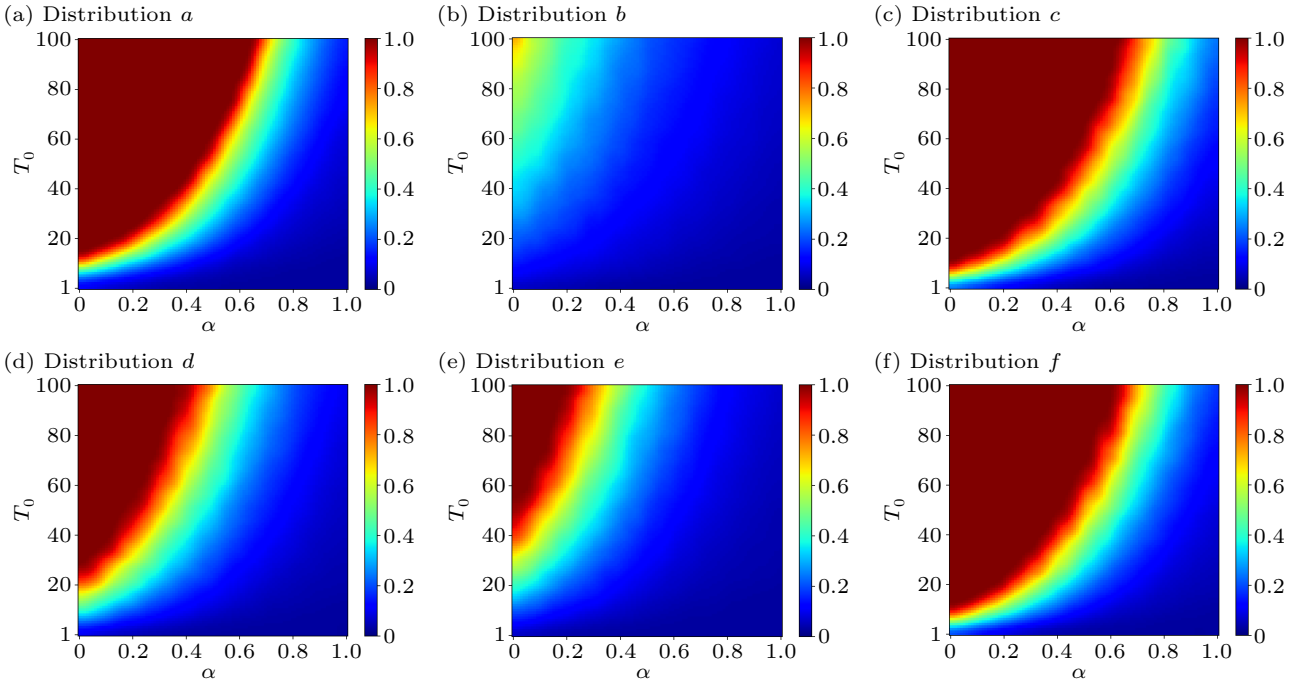


Fig. 10. The dependence of λ_c on α and T_0 for distributions a–f.

4.3. Social contagions with adoption thresholds correlated with degrees

Figure 11 shows the simulation results of $R(\infty)$ on the λ–β plane for different α. Note that here we only consider the case where $\beta \in [-1, 1]$ to simplify the study. In each subgraph, the region with $R(\infty) > 0$ for $\beta > 0$ is always larger than that for $\beta < 0$, indicating that it is more favorable for social contagions when adoption thresholds are positively correlated with degrees. From Fig. 11(a), we can see that social contagions hardly break out when α is relatively small. From Figs. 11(a)–11(f), we find that $R(\infty)$ for different β with an identical λ is getting closer as α increases, and when $\alpha = 1.1$, the effects of β on social contagions almost disappear. This result shows that the increasing of α suppresses the effects of adoption thresholds' heterogeneity on social contagions once again. Additionally, we find a crossover phenomenon in phase transition in Fig. 11(b), while in the other subgraphs, there is no crossover phenomenon in phase transition. This indicates that α can also influence the phase transition types under some specific conditions. The different phase transition regions of Fig. 11(b) are separated by the vertical white dashed line. In region I, $R(\infty)$ decreases continuously with β, which shows a second-order phase transition, while in region II, $R(\infty)$ decreases discontinuously with β, showing a first-order phase transition.

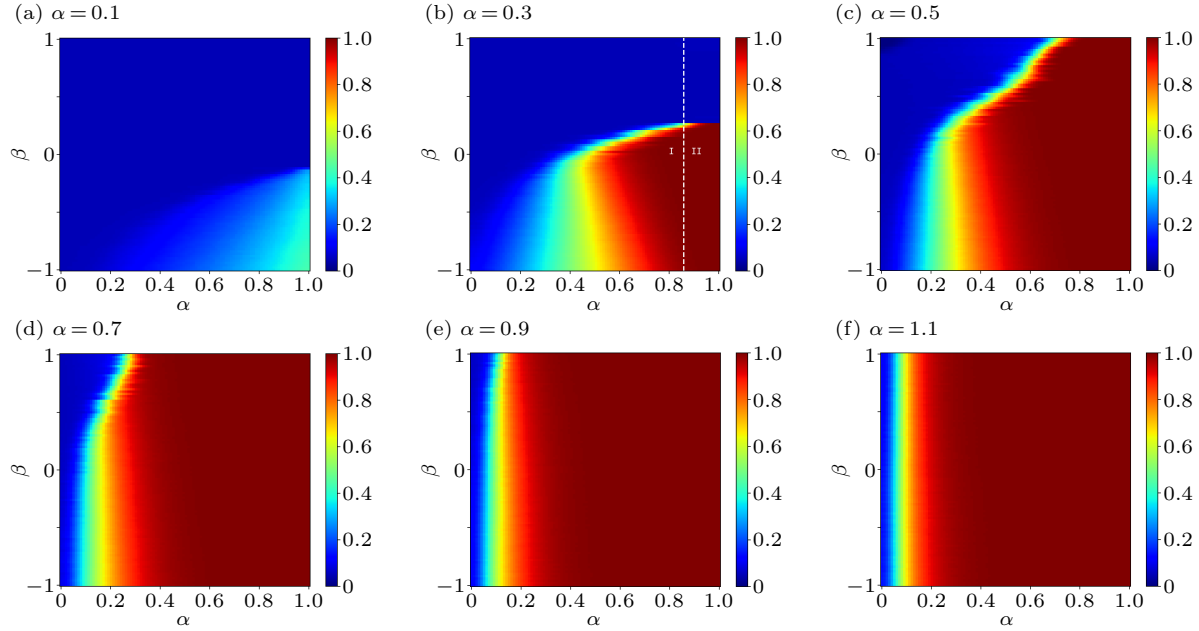


Fig. 11. The dependence of $R(\infty)$ on λ and β for (a) $\alpha = 0.1$, (b) $\alpha = 0.3$, (c) $\alpha = 0.5$, (d) $\alpha = 0.7$, (e) $\alpha = 0.9$, and (f) $\alpha = 1.1$.

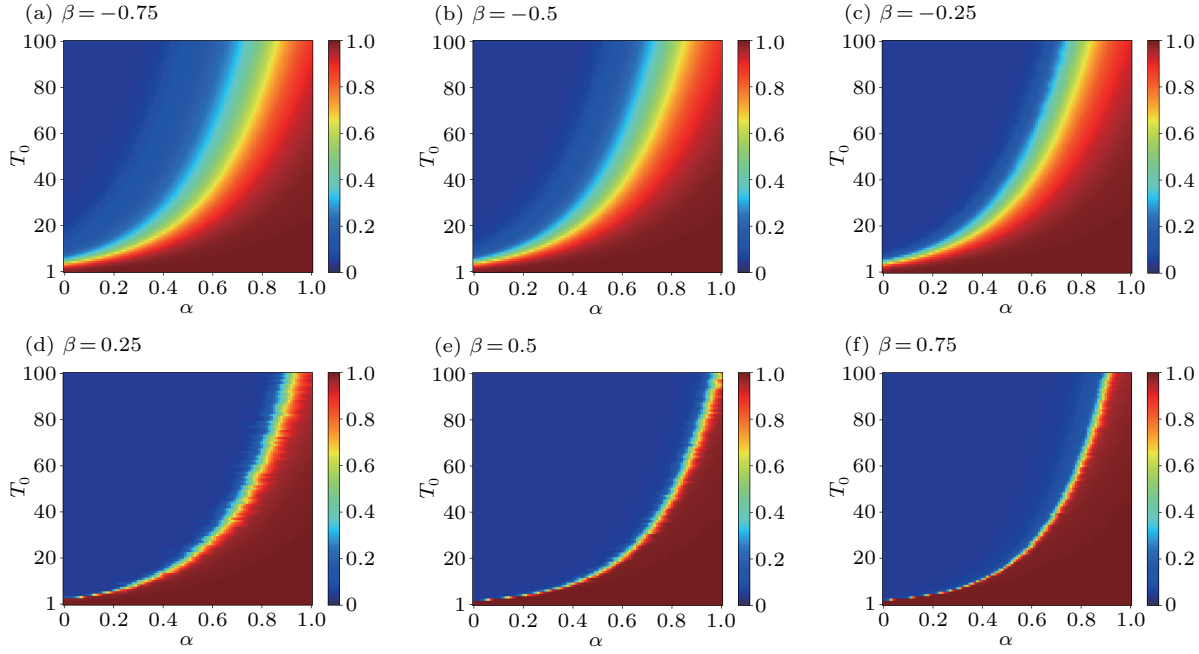


Fig. 12. The dependence of $R(\infty)$ on α and T_0 for (a) $\beta = -0.75$, (b) $\beta = -0.5$, (c) $\beta = -0.25$, (d) $\beta = 0.25$, (e) $\beta = 0.5$, and (f) $\beta = 0.75$ while $\lambda = 0.5$.

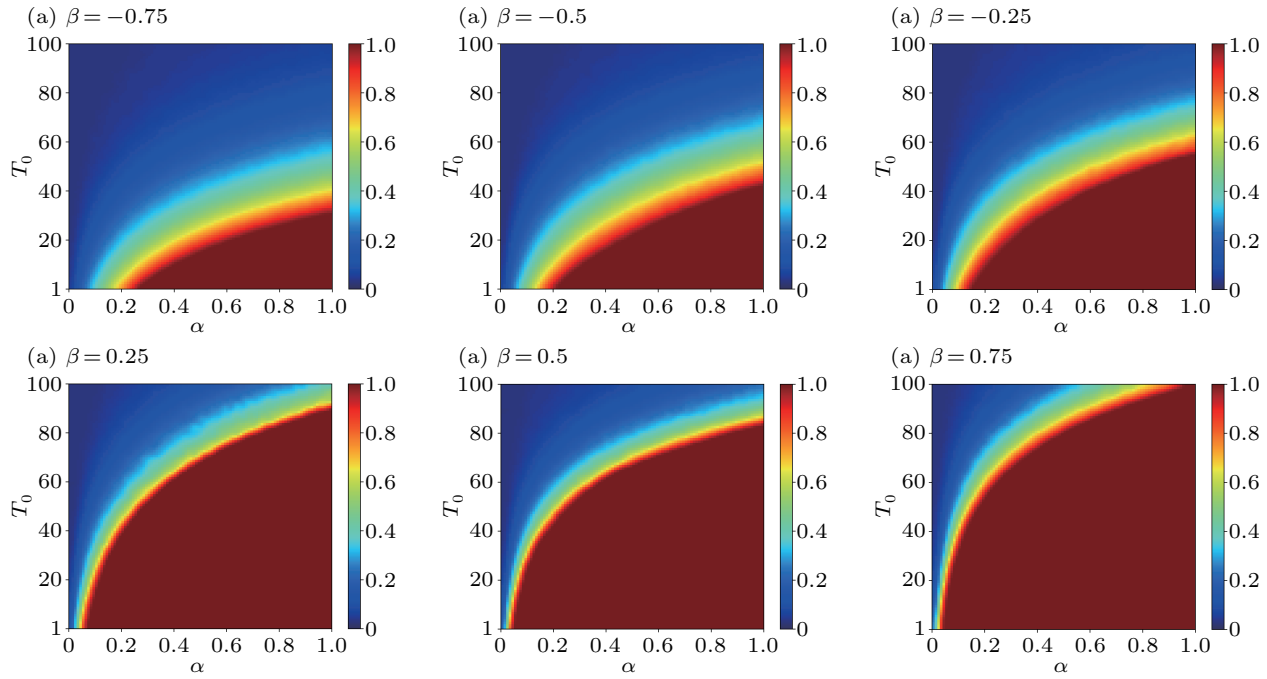


Fig. 13. The dependence of λ_c on α and T_0 for (a) $\beta = -0.75$, (b) $\beta = -0.5$, (c) $\beta = -0.25$, (d) $\beta = 0.25$, (e) $\beta = 0.5$, and (f) $\beta = 0.75$.

Figure 12 shows the simulation results of $R(\infty)$ on the α–T_0 plane for different β, while Fig. 13 shows the simulation results of λ_c on the α–T_0 plane for different β. It is more favorable for social contagions when adoption thresholds are negatively correlated with degrees, which is supported by the following: In Fig. 12, the region in color red for $\beta < 0$ is larger than that for $\beta > 0$, indicating that it is easier to achieve global spreading when adoption thresholds are negatively correlated with degrees. In Fig. 13, the region in blue for $\beta < 0$ is larger than that for $\beta > 0$, indicating that outbreaks occur more easily when adoption thresholds are positively correlated with degrees.

As for phase transition, in Fig. 12, crossover phenomena in phase transition are observed when $\beta > 0$: When α is relatively low, $R(\infty)$ decreases discontinuously with T_0, showing a first-order phase transition. As α increase, the phase transition type will change to second-order, and $R(\infty)$ decreases continuously with T_0. However, in Fig. 13, no crossover phenomena are observed when $\beta < 0$ or $\beta > 0$.

5. Conclusions

This paper proposes an improved threshold model for social contagions considering both heterogeneous social influence and heterogeneous adoption thresholds. Referring to the edge-based compartmental theory and the heterogeneous mean-field theory, a generalized edge-based compartmental theory which considers the heterogeneity of social influence and adoption thresholds is developed for theoretical analysis. Then, we investigate the social contagions with adoption thresholds following normal distributions, the effects of various threshold distributions on social contagions, and the social contagions with adoption thresholds correlated with degrees, respectively. The main conclusions are shown as follows.

The results indicate that the heterogeneity of both social influence and adoption thresholds will promote social contagions. Since the actual social influence and adoption thresholds are heterogeneous, this explains the reason why social contagions spread widely and fast. In investigating the relationship of $R(\infty)$ versus λ, the increasing α suppresses the effects of adoption thresholds' heterogeneity, and when α is large enough, the effects disappear. Specifically, in the case that adoption thresholds follow normal distributions, the increasing α suppresses the effects of σ on the relationship. In investigating the effects of various threshold distributions on social contagions, the increasing α suppresses the effects of threshold distribution types on the relationship. When adoption thresholds are correlated with degrees, the increasing α suppresses the effects of β on the relationship. The rationale for these phenomena is briefly analyzed in this paper. As for phase transition type, there is no crossover phenomena found when investigating λ_c on the α–T_0 plane. In investigating $R(\infty)$ on the α–T_0 plane, crossover phenomena in phase transition occur when adoption thresholds are homogeneous, adoption thresholds follow a power-low distribution, $F(T)$ increases linearly with increasing T, and adoption thresholds are positively correlated with degrees. In these crossover phenomena, when α is relatively small, $R(\infty)$ decreases discontinuously with T_0, and phase transition type is first-order. While λ is sufficiently large, $R(\infty)$ decreases continuously with T_0, and the phase transition type changes to second-order. Besides, in investigating $R(\infty)$ on the λ–β plane, when $\alpha = 0.3$,

crossover phenomena in phase transition occur. When λ is relatively small, $R(\infty)$ decreases continuously with β, which shows a second-order phase transition. While λ is sufficiently large, $R(\infty)$ decreases discontinuously with β, showing a first-order phase transition. The theoretical predictions agree well with the simulation results, demonstrating the validity of the theoretical analysis proposed in this paper.

This paper investigates the effects of individual heterogeneity on social contagions, and the results may help to understand the complexity of social contagions. The findings in this paper can be regarded as a supplement to those of previous research, as well as a reference for future research. However, there are still many improvements that can be done in future work. The social influence in reality is not only just correlated with degrees, but can be strongly affected by high-order structures, such as community structures,[29–31] multi-relational networks,[32,33] multi-layer networks,[34,35] and high-order networks.[36,37] Besides, apart from the topology factors of networks, individuals' psychological factors[38,39] on social influence are indispensable. In addition, the effects of other types of adoption thresholds on social contagions are also worthy of investigation.

Acknowledgment

Project supported by the National Natural Science Foundation of China (Grant Nos. 62266030 and 61863025).

References

[1] Mønsted B, Sapieżyński P, Ferrara E and Lehmann S 2017 *PloS One* **12** e0184148
[2] Lü L, Chen D B and Zhou T 2011 *New J. Phys.* **13** 123005
[3] Centola D and Macy M 2007 *American Journal of Sociology* **113** 702
[4] Zheng M, Lü L, Zhao M, *et al.* 2013 *Phys. Rev. E* **88** 012818
[5] Karsai M, Iniguez G, Kaski K and Kertész J 2014 *J. Roy. Soc. Inter.* **11** 20140694
[6] Traag V A 2016 *PloS One* **11** e0153539
[7] Granovetter M S 1973 *American Journal of Sociology* **78** 1360
[8] Watts D J 2002 *Proc. Natl. Acad. Sci. USA* **99** 5766
[9] Majdandzic A, Podobnik B, Buldyrev S V, Kenett D Y, Havlin S and Eugene Stanley H 2014 *Nat. Phys.* **10** 34
[10] Wang W, Shu P, Zhu Y X, Tang M and Zhang Y C 2015 *Chaos* **25** 103102
[11] Podobnik B, Horvatic D, Lipic T, Perc M, Buldu J M and Stanley H E 2015 *J. Roy. Soc. Inter.* **12** 20150770
[12] Han L, Lin Z, Tang M, Zhou J, Zou Y and Guan S 2020 *Phys. Rev. E* **101** 042308
[13] Miller J C 2007 *Phys. Rev. E* **76** 010101
[14] Yang H, Tang M and Gross T 2015 *Sci. Rep.* **5** 13122
[15] Cui A X, Wang W, Tang M, Fu Y, Liang X and Do Y 2014 *Chaos* **24** 033113
[16] Jo H H, Perotti J I, Kaski K and Kertész J 2014 *Phys. Rev. X* **4** 011041
[17] Zhu Y X, Wang W, Tang M and Ahn Y Y 2017 *Phys. Rev. E* **96** 012306
[18] Wang W, Chen X L and Zhong L F 2018 *Physica A* **503** 604
[19] Wang W, Tang M, Shu P and Wang Z 2016 *New J. Phys.* **18** 013029
[20] Karampourniotis P D, Sreenivasan S, Szymanski B K and Korniss G 2015 *PloS one* **10** e0143020
[21] Watts D J and Dodds P S 2007 *Journal of Consumer Research* **34** 441
[22] Wang Q, Wang H, Zhang Z, Li Y, Liu Y and Perc M 2018 *Physica A* **502** 570
[23] Chen W, Wang Y and Yang S 2009 *Proceedings of the 15th ACM SIGKDD international conference on Knowledge discovery and data mining* pp. 199–208
[24] Wang W, Tang M, Zhang H F, Gao H, Do Y and Liu Z H 2014 *Phys. Rev. E* **90** 042803
[25] Miller J C 2011 *Journal of Mathematical Biology* **62** 349
[26] Pastor-Satorras R and Vespignani A 2002 *Phys. Rev. E* **65** 035108
[27] Castellano C and Pastor-Satorras R 2006 *Phys. Rev. Lett.* **96** 038701
[28] Wang W, Tang M, Zhang H F and Lai Y C 2015 *Phys. Rev. E* **92** 012820
[29] Shi D, Shang F, Chen B, Expert P, Lü L, Yang A, Stanley H E, Lambiotte R, Evans T S and Li R 2022 arXiv:2209.15497
[30] Bovet A and Makse H A 2022 *Encyclopedia of Complexity and Systems Science* pp. 1–11
[31] Newman M E 2006 *Phys. Rev. E* **74** 036104
[32] Li R Q, Ming T and Pak-Ming H 2013 *Acta Phys. Sin.* **62** 168903 (in Chinese)
[33] Nian F and Yao S 2018 *Applied Mathematics and Computation* **339** 866
[34] Salehi M, Sharma R, Marzolla M, Magnani M, Siyari P and Montesi D 2015 *IEEE Transactions on Network Science and Engineering* **2** 65
[35] Bródka P, Musial K and Jankowski J 2020 *IEEE Access* **8** 10316
[36] Majhi S, Perc M and Ghosh D 2022 *J. Roy. Soc. Inter.* **19** 20220043
[37] Chowdhary S, Kumar A, Cencetti G, Iacopini I and Battiston F 2021 *Journal of Physics: Complexity* **2** 035019
[38] Huo L and Ma C 2018 *Discrete Dynamics in Nature and Society* **2018** 9314907
[39] Xu H, Li T, Liu X, Liu W and Dong J 2019 *Physica A* **525** 234